

Antifungal activity and mode of action of silver nano-particles on *Candida albicans*

Keuk-Jun Kim · Woo Sang Sung · Bo Kyoung Suh ·
Seok-Ki Moon · Jong-Soo Choi · Jong Guk Kim ·
Dong Gun Lee

Received: 22 October 2007 / Accepted: 4 August 2008 / Published online: 4 September 2008
© Springer Science+Business Media, LLC. 2008

Abstract In this study, the antifungal effects of silver nano-particles (nano-Ag) and their mode of action were investigated. Nano-Ag showed antifungal effects on fungi tested with low hemolytic effects against human erythrocytes. To elucidate the antifungal mode of action of nano-Ag, flow cytometry analysis, a glucose-release test, transmission electron microscopy (TEM) and the change in membrane dynamics using 1,6-diphenyl-1,3,5-hexatriene (DPH), as a plasma membrane probe, were performed with *Candida albicans*. The results suggest nano-Ag may exert an antifungal activity by disrupting the structure of the cell membrane and inhibiting the normal budding process due to the destruction of the membrane integrity. The present study indicates nano-Ag has considerable antifungal activity, deserving further investigation for clinical applications.

Keywords Silver nano-particles · Antifungal activity · *Candida albicans* · Membrane disruption

Introduction

In recent years, a rapid increase in microbes that are resistant to conventionally-used antibiotics has been observed (Goffeau 2008). Antifungal drug therapy is no exception; resistance too many of the antifungal agents now in use has emerged. Although antifungal-drug resistance does not seem to be as much of a problem as resistance to antibacterial agents in bacteria, one long-term concern is that the number of fundamentally different types of antifungal agents that are available for treatment remains extremely limited. This is because fungi are eukaryotic organisms with a structure and metabolism that are similar to those of eukaryotic hosts. Therefore, there is an inevitable and urgent medical need for antibiotics with novel antimicrobial mechanisms.

Since ancient times it has been known that silver and its compounds are effective antimicrobial agents (Silver 2003; Klasen 2000). In particular, due to the recent advances in research on metal nanoparticles, nano-Ag has received special attention as a possible antimicrobial agent (Baker et al. 2005; Melaiye et al. 2005; Sondi and Salopek-Sondi 2004). Therefore, the preparation of uniform nanosized silver particles with

K.-J. Kim and W. S. Sung contributed equally to this work and should be considered co-first authors.

K.-J. Kim · W. S. Sung · B. K. Suh · J. G. Kim ·
D. G. Lee (✉)
Department of Microbiology, College of Natural
Sciences, Kyungpook National University,
1370 Sankyuk-dong, Puk-ku, Daegu 702-701,
South Korea
e-mail: dglee222@knu.ac.kr

S.-K. Moon · J.-S. Choi
Department of Dermatology, College of Medicine,
Yeungnam University, Daegu, South Korea

specific requirements in terms of size, shape, and physical and chemical properties is of great interest in the formulation of new pharmaceutical products (Merisko-Liversidge et al. 2003; Brigger et al. 2002). Though the biocidal effect and mode of action of silver ion are known, nevertheless, the antifungal effects and the mode of action of nano-Ag against fungi have remained mostly unknown. This study reports on the antifungal effects and mode of action of nano-Ag.

Materials and methods

Materials

Amphotericin B, carbonyl cyanide *m*-chlorophenylhydrazone (CCCP), trehalase and RNase A were purchased from the Sigma Chemical Co. Stock solutions of amphotericin B were prepared in dimethyl sulfoxide (DMSO), and stored at -20°C . For all the experiments, a final concentration of 2% DMSO was used as the solvent carrier.

Preparation of nano-Ag

One-hundred grams of solid silver were dissolved in 100 ml of 100% nitric acid at 90°C , and then 1 l of distilled water was added. By adding sodium chloride to the silver solution, the Ag ions were precipitated and then clustered together to form monodispersed nanoparticles in the aqueous medium. The sizes and morphology of nano-Ag were examined by using a transmission electron microscope (H-7600, HITACHI, LTD). The results showed that nano-Ag was a spherical form and its average size was 3 nm (Fig. 1). Because the final concentration of colloidal silver was 60,000 ppm, this solution was diluted, and then samples of different concentrations were used to investigate the antifungal effects of nano-Ag.

Microorganisms and culture conditions

Saccharomyces cerevisiae (KCTC 7296), and *Trichosporon beigelii* (KCTC 7707) were obtained from the Korean Collection for Type Cultures (KCTC) of the Korea Research Institute of Bioscience and Biotechnology (KRIBB). *Candida albicans* (ATCC 90028) was obtained from the American Type Culture

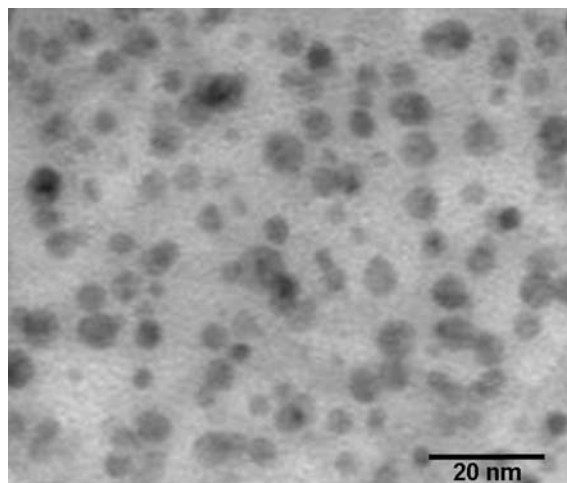


Fig. 1 Transmission electron micrograph of the silver nanoparticles (nano-Ag) used in this work. The bar marker represents 20 nm

Collection (ATCC). Fungal cells were cultured in a YPD broth (Difco) containing yeast extract, peptone, and dextrose (50 g/l) with aeration at 28°C .

Determination of antifungal susceptibility

Fungal cells ($2 \times 10^4/\text{ml}$) were inoculated into a YPD broth and dispensed 0.1 ml/well into microtiter plates. MICs were determined by a serial 2-fold dilution of test compounds, following a micro-dilution method (Lee et al. 2003) and MTT (3-(4,5-dimethyl-2-thiazolyl)-2,5-diphenyl-2H-tetrazolium bromide) assay (Sung et al. 2007). After 48 h of incubation at 28°C , the minimal compound concentrations were defined as the lowest concentrations which inhibited 90% of the growth compared with that of the growth control. Growth was assayed with a microtiter ELISA Reader by monitoring absorption at 580 nm. MIC values were determined by three independent assays.

Hemolytic activity against human erythrocytes

The hemolytic effects of nano-Ag were examined by measuring the release of hemoglobin from a 4% suspension of fresh human red blood cells (hRBCs). The hRBCs were washed three times with a phosphate-buffered saline (PBS: 35 mM phosphate buffer/150 mM NaCl, pH 7.4). One-hundred microliters of a hRBC suspension were added to the 96-well microtiter plates, and then 100 μl of the compound solution

in a PBS were mixed into each well. After incubating the mixtures for 1 h at 37°C, the mixtures were centrifuged at 1,500 rpm for 10 min, and the aliquots were transferred to new 96-well microtiter plates. The absorbance of the aliquots was measured at 414 nm by using a microtiter ELISA Reader. Hemolytic rates of 0 and 100% were determined in a PBS and 0.1% Triton X-100, respectively (Park et al. 2003). The percentage of hemolysis was calculated by employing the following equation: Percentage hemolysis = $[(\text{Abs}_{414 \text{ nm}} \text{ in the compound solution} - \text{Abs}_{414 \text{ nm}} \text{ in a PBS}) / (\text{Abs}_{414 \text{ nm}} \text{ in 0.1\% Triton X-100} - \text{Abs}_{414 \text{ nm}} \text{ in a PBS})] \times 100$.

Flow cytometric analysis for plasma membrane potential

For analysis of the membrane integrity after the nano-Ag treatment, Log-phased cells of *C. albicans* (1×10^8 cells), cultured in a YPD medium, were harvested and resuspended with 1-ml of a fresh YPD medium, containing 30 µg/ml of nano-Ag (at 15 times the MIC) or 10 µM of CCCP used as a positive control. After incubation for 3 h, the cells were washed three times with a PBS. To detect any depolarization of the cell membrane, 1-ml of a PBS, containing 50 µg of bis-(1,3-Dibutylbarbituric Acid) Trimethine Oxonol [DiBAC₄(3)], was added and the samples were incubated for 1 h at 4°C in the dark (Liao et al. 1999). Flow cytometric analysis was performed via a FACSCalibur flow cytometer.

Measurement of plasma membrane fluorescence anisotropy

The anisotropy of fluorescence from exponential *C. albicans* cells labeled by 1,6-diphenyl-1,3,5-hexatriene (DPH) was used to monitor changes in membrane dynamics. The cells (1×10^8 cells in a YPD medium), containing 20, 40, 60 and 80 µg/ml of nano-Ag or amphotericin B, were incubated at a physiological temperature of 28°C on a rotary shaker at 140 rpm for 2 h. The control cells were incubated without a compound. The cells were fixed with formaldehyde (0.37% v/v) for 45 min and they were collected by centrifugation at 3,000 rpm, then washed several times with a PBS buffer (pH 7.4), and the pellets were frozen in liquid nitrogen. For DPH labeling, the pellets were resuspended in a PBS buffer

and incubated at 28°C for 45 min in the presence of 0.6 mM of DPH, followed by several washings in a PBS buffer. The steady-state fluorescence anisotropy was measured using a SHIMADZU RF-5301PC spectrofluorometer at 350 nm excitation and 425 nm emission wavelengths (Fernandes et al. 2000). The results represent the average of the triplicate measurements from three independent assays.

Determining released glucose and trehalose

Fungal strains were grown at 28°C in a YPD medium. *C. albicans* cells were washed three times with a PBS, and then 1 ml of the *C. albicans* cell suspension (1×10^8 cells), containing 20 µg/ml of nano-Ag (at 20 times the MIC), was incubated for 2 h at 28°C in a PBS. The negative control was incubated without nano-Ag, and a positive control was incubated with 100 µg/ml of amphotericin B (at 20 times the MIC). The fungal cells were settled by centrifugation (12,000 rpm for 20 min). The pellets were dried to calculate their dry weight and supernatants were transferred to a new tube. Released glucose and trehalose-containing supernatants were added to 0.05 units of trehalase. After 1 h of enzymatic reaction at 37°C, the reaction suspension was mixed with water and 16% DNS reagent (3,5-Dinitrosalicylic acid 1%, NaOH 2%, Sodium potassium tartrate 20%) was added. For the reaction of glucose with the DNS reagent, the mixture was boiled for 5 min and cooled. Color formations were measured at 525 nm. The results represent the average of the measurements conducted in triplicate of three independent assays.

Transmission electron microscopy (TEM)

Log-phased cells of *C. albicans* (1×10^8 cells) cultured in a YPD medium, were harvested and incubated in the presence of several amounts of nano-Ag for 24 h at 28°C. TEM was used as a complementary technique to examine sections of the treated cells, using standard procedures for fixing and embedding sensitive biological samples, which are described elsewhere (Osuni 1998; Mares et al. 1998).

Flow cytometric analysis for a fungal cell cycle

Log-phased cells of *C. albicans* (1×10^8 cells) cultured in a YPD medium, were harvested and

treated with 40 $\mu\text{g/ml}$ of nano-Ag (at 20 times the MIC). After incubation for 8 h, the cells were washed with a PBS and fixed with 70% ethanol overnight at 4°C. The cells were treated with 200 $\mu\text{g/ml}$ of RNase A and the mixture was left to react for 2 h at 37°C. For DNA staining, 50 $\mu\text{g/ml}$ of propidium iodide were added and incubated for 1 h at 4°C in the dark (Green et al. 1999). Flow cytometric analysis was performed by a FACSCalibur flow cytometer. The values represent the average of the measurements conducted in triplicate of three independent assays.

Results

In vitro antifungal activity

In this study, amphotericin B, an antifungal agent which is widely used to treat serious systemic infections, was used as a positive control to compare with nano-Ag (Hartsel and Bolard 1996). These strains, such as *C. albicans* and *T. beigelii*, exist as a commensal of humans and are superficial contaminants that can cause a variety of serious infections in humans. *S. cerevisiae* is a universal yeast strain which has been studied regarding the effects of drugs against yeast strains. Nano-Ag showed antifungal activity against fungal strains tested. Nano-Ag exhibited a MIC value of 2 $\mu\text{g/ml}$, and the MIC values of this compound were approximately the same level as those of amphotericin B, showing MIC values of 2.5–5 $\mu\text{g/ml}$ toward the fungal strains tested. To assess

the cytotoxicity of nano-Ag against human erythrocytes, the hemolytic activity was evaluated by the percentage of hemolysis at the concentration range 1.25–10 $\mu\text{g/ml}$ of nano-Ag. Nano-Ag caused 6% lysis of erythrocytes at a concentration of 10 $\mu\text{g/ml}$, while amphotericin B caused 10% lysis at the same level.

Flow cytometric analysis for plasma membrane potential

To assess whether nano-Ag can affect the function of a fungal plasma membrane, the dissipation of the fungal plasma membrane potential was investigated. *C. albicans* cells were cultured in the presence of nano-Ag or CCCP used as a positive control, and the amounts of accumulated DiBAC₄(3) in the cells were measured via flow cytometry by staining with DiBAC₄(3). DiBAC₄(3) has a high voltage sensitivity and it enters depolarized cells, where it binds to lipid-rich intracellular components (Liao et al. 1999). Therefore, the fluorescence of DiBAC₄(3) increases upon membrane depolarization. The addition of nano-Ag to *C. albicans* cells caused an increase in fluorescence intensity, similar to the increase observed in the presence of CCCP, which is indicative of membrane depolarization (Fig. 2).

Change in the plasma membrane dynamics of fungal cells

The effect of nano-Ag on the fungal plasma membrane was further investigated by using DPH as a

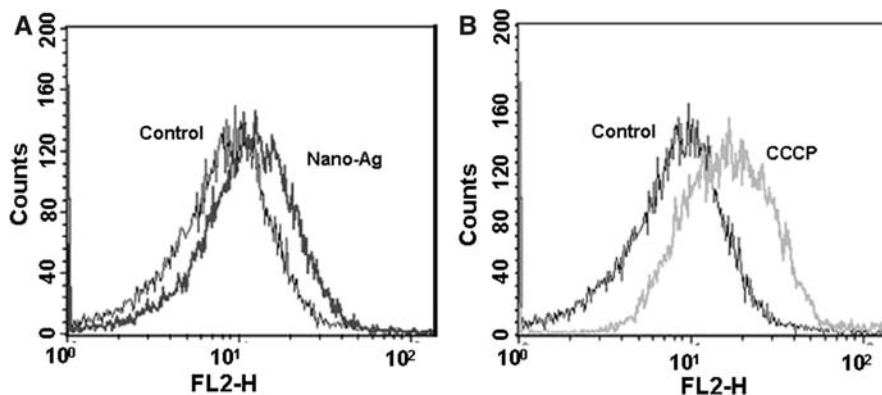


Fig. 2 FACS analysis of DiBAC₄(3) staining in *C. albicans*. *C. albicans* were mixed with 30 $\mu\text{g/ml}$ of nano-Ag and 10 μM of CCCP and incubated at 28°C for 3 h under constant shaking. This figure showed the fluorescence intensity

of stained after *C. albicans* were treated with compounds. FL2-H indicates the log fluorescent intensity of DiBAC₄(3), and y-axis indicates cell number (events): (a) treated with nano-Ag, (b) treated with CCCP

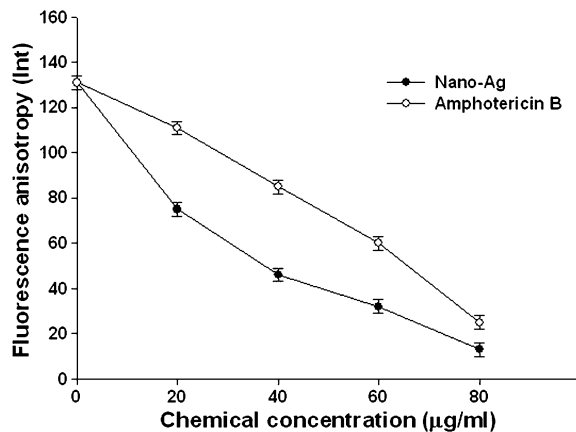


Fig. 3 DPH fluorescence anisotropy after the addition of nano-Ag and amphotericin B. Treatment with 20, 40, 60 and 80 µg/ml of nano-Ag or amphotericin B, and the error bars represent the standard deviation (SD) values for three independent experiments, performed in triplicate

membrane probe. If the antifungal activities exerted by nano-Ag on *C. albicans* are at the level of the plasma membrane, DPH, which interacts with an acyl group of the plasma membrane lipid bilayer, could not be inserted into the membrane. As shown in Fig. 3, the plasma membrane DPH fluorescence anisotropy was significantly decreased by increasing the concentrations of nano-Ag and amphotericin B. This is consistent with the disruption of the plasma membrane by nano-Ag as well as by a positive control, amphotericin B.

Intracellular glucose and trehalose release

The ability of nano-Ag to disturb the integrity of the plasma membrane of fungal cells was also assessed by measuring the glucose and trehalose released in cell suspensions which were exposed to this compound. *C. albicans* cells were cultured in the presence of nano-Ag or amphotericin B and the amounts of released glucose and trehalose were investigated. The results showed that nano-Ag or amphotericin B-treated cells both accumulated more intracellular glucose and trehalose than the compound-untreated cells. In addition, these cells also increased more extracellular glucose and trehalose than the compound-untreated cells. The extracellular glucose and trehalose, induced by amphotericin B, were measured as being 27.4 µg per fungal dry weight of 1 mg. The extracellular glucose and trehalose amounts, however, induced by

Table 1 The concentrations of trehalose and glucose from *C. albicans* by nano-Ag and amphotericin B

	Amounts of trehalose and glucose concentrations (µg/mg)	
	Intracellular glucose and trehalose	Released glucose and trehalose
Control	7.2	6.8
Nano-Ag	16.1	30.3
Amphotericin B	20.5	27.4

nano-Ag were measured as being 30.3 µg per fungal dry weight of 1 mg. This rate was significantly higher than that induced in the compound-untreated cells (Table 1).

Transmission electron microscopic analysis

TEM was used to evaluate the ability of nano-Ag to disrupt the fungal envelope structure. The results showed that the treated fungal cells showed significant damage, which was characterized by the formation of a “pit” in their cell walls and pores in their plasma membrane (Fig. 4).

The arrest of fungal cell cycle

To understand how the activity of nano-Ag affects intracellular physiology, the effects on the cell cycle progress of *C. albicans* were further investigated. The cells were cultured in the presence or absence of nano-Ag and their DNA content was determined *via* flow cytometry by staining with propidium iodide (PI). PI is a DNA-staining dye that intercalates between the bases of DNA or RNA molecules (Tas and Westerneng 1981). As shown in Fig. 5, the percentage of cells in the G₂/M phase increased by 15%, while that in the G₁ phase significantly decreased by about 20% in the presence of nano-Ag.

Discussion

Nanosized inorganic particles represent an increasingly important material in the development of novel nanodevices which can be used in numerous physical, biological, biomedical, and pharmaceutical applications (Chan et al. 2002; Sondi et al. 2000). In particular, nano-Ag has good a possibility as an

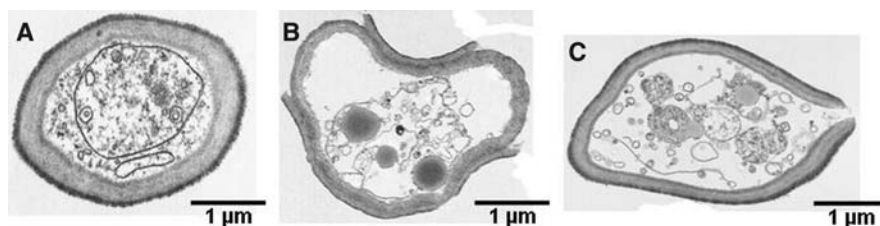


Fig. 4 Transmission electron micrograph of *C. albicans* cells. *C. albicans* were incubated in the presence of several amounts of nano-Ag for 24 h at 28°C. The bar marker represents 1 µm:

(a) control with no nano-Ag, (b) treated with 170, (c) 400 µg/ml of nano-Ag

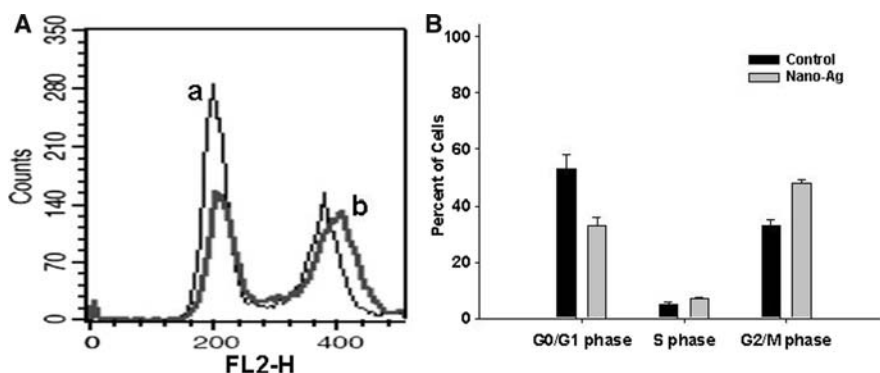


Fig. 5 The effects of nano-Ag on the process of the cell cycle of *C. albicans*. *C. albicans* were incubated in the presence of nano-Ag for 8 h at 28°C. FL2-H indicates the fluorescent intensity of PI, and y-axis indicates cell number (events): (a)

the FACS diagram of cell cycle, (b) a histogram of percentage of cell cycle. (a) Control without nano-Ag, (b) cells of 40 µg/ml nano-Ag treatment

antimicrobial agent, since it is highly toxic to most microorganisms (Zhao and Stevens 1998; Herrera et al. 2001), while just a few rare strains are silver-resistant (Klaus et al. 1999). To use nano-Ag as an antimicrobial agent, it is essential to know the mechanism of the antimicrobial effect. Even though some researchers have investigated the mechanism of the antibacterial effect of nano-Ag on bacterial model including *E. coli*, the mode of their antifungal action has remained mostly unknown.

In this study, the antifungal activity of nano-Ag toward *C. albicans* as a model for fungi was investigated. Nano-Ag exhibited a potent antifungal activity against fungal strains tested, similar to the antifungal activity in the MIC values of amphotericin B, which was used as a positive control. These results indicated that nano-Ag has remarkable potential as an antifungal agent in treating fungal infectious diseases. Many antimicrobial agents are limited in clinical applications, as they bring about cytolysis of human erythrocytes. Nano-Ag shows low hemolytic activity, while amphotericin B shows a slightly higher

hemolytic activity than that of nano-Ag that could be fatal in patients who are treated via this agent for fungal infections. This result confirms the antifungal effects of nano-Ag, on human erythrocytes with either no effect or a weakly cytolytic effect.

To provide information on the mode of action of nano-Ag, its ability to dissipate the membrane potential of *C. albicans* was investigated (Fig. 2). These results indicated that nano-Ag affected yeast cells by attacking their membranes, thus disrupting membrane potential. Nano-Ag was also measured for its ability to affect membrane dynamics (Fig. 3). In this assay, amphotericin B was used as a positive control. In general, amphotericin B binds to membrane sterols and transmembrane pores are formed, thus causing a leakage of cell constituents and eventually cell death (Fujii et al. 1997). Here, these data were used to assess the global “rigidity” of the plasma membrane through the contrast between nano-Ag and amphotericin B. This decrease in the amount of DPH, after treatment, provides further evidence that nano-Ag act on the plasma membrane. Fungal cells maintain

their membrane potential by establishing multiple ion gradients across the cytoplasmic membrane. Since the proper maintenance of intracellular components is important to fungal viability, the glucose and trehalose release was measured during exposure to nano-Ag in *C. albicans* (Fig. 4). Trehalose can protect proteins and biological membranes from inactivation or denaturation caused by a variety of stress conditions, including desiccation, dehydration, heat, cold, oxidation, and toxic agents in yeast (Alvarez-Peral et al. 2002; Elbein et al. 2003). The analysis of glucose and trehalose release, during nano-Ag exposure, suggests that it may be one of several intracellular components released during membrane disruption by nano-Ag (Table 1). As for the mechanism by which nano-Ag breaks down the membrane permeability barrier, it is possible that nano-Ag perturbs the membrane lipid bilayers, causing the leakage of ions and other materials as well as forming pores and dissipating the electrical potential of the membrane. Additionally, TEM analysis confirms the interaction between nano-Ag and the membrane structure. *C. albicans* cells, during nano-Ag exposure, show significant changes to their membranes, which are recognized by the formation of “pits” on their surfaces, and finally, result in the formation of pores and cell death (Fig. 4).

To elucidate the physiological changes of the fungal cells induced by nano-Ag, a flow cytometric analysis of the cell cycle was performed. The results showed that nano-Ag arrested the cell cycle at the G₂/M phase in *C. albicans* (Fig. 5). These data suggest that nano-Ag inhibited some cellular processes which are involved in normal bud growth. Endo et al. have reported that the inhibition of bud growth correlates with membrane damage (Endo et al. 1997). This report suggests that nano-Ag inhibits the normal budding process, probably through the destruction of membrane integrity.

In summary, nano-Ag exhibited potent antifungal effects on fungi tested, probably through destruction of membrane integrity; therefore, it was concluded that nano-Ag has considerable antifungal activity, deserving further investigation for clinical applications.

References

- Alvarez-Peral FJ, Zaragoza O, Pedreno Y, Argüelles J (2002) Protective role of trehalose during severe oxidative stress caused by hydrogen peroxide and the adaptive oxidative stress response in *Candida albicans*. Microbiology 148: 2599–2606
- Baker C, Pradhan A, Pakstis L, Pochan DJ, Shah SI (2005) Synthesis and antibacterial properties of silver nanoparticles. J Nanosci Nanotechnol 5:244–249. doi:10.1166/jnn.2005.034
- Brigger I, Dubernet C, Couvreur P (2002) Nanoparticles in cancer therapy and diagnosis. Adv Drug Deliv Rev 54:631–651. doi:10.1016/S0169-409X(02)00044-3
- Chan WCW, Maxwell DJ, Gao X, Bailey RE, Han M, Nie S (2002) Luminescent quantum dots for multiplexed biological detection and imaging. Curr Opin Biotechnol 13:40–46. doi:10.1016/S0958-1669(02)00282-3
- Elbein AD, Pan YT, Pastuszak I, Carroll D (2003) New insights on trehalose: a multifunctional molecule. Glycobiology 13:17R–27R. doi:10.1093/glycob/cwg047
- Endo M, Takesako K, Kato I, Yamaguchi H (1997) Fungicidal action of aureobasidin A, a cyclic depsipeptide antifungal antibiotic, against *Saccharomyces cerevisiae*. Antimicrob Agents Chemother 41:672–676
- Fernandes AR, Prieto FM, Sa-Correia I (2000) Modification of plasma membrane lipid order and H⁺-ATPase activity as part of the response of *Saccharomyces cerevisiae* to cultivation under mild and high copper stress. Arch Microbiol 173:262–268. doi:10.1007/s002030000138
- Fujii G, Chang J, Coley T, Steere B (1997) The formation of amphotericin B ion channels in lipid bilayers. Biochemistry 36:4959–4968. doi:10.1021/bi962894z
- Goffeau A (2008) Drug resistance: the fight against fungi. Nature 452:541–542. doi:10.1038/452541a
- Green LJ, Marder P, Mann LL, Chio LC, Current WL (1999) LY303366 exhibits rapid and potent fungicidal activity in flow cytometric assays of yeast viability. Antimicrob Agents Chemother 43:830–835
- Hartel S, Bolard J (1996) Amphotericin B: new life for an old drug. Trends Pharmacol Sci 17:445–449. doi:10.1016/S0165-6147(96)01012-7
- Herrera M, Carrion P, Baca P, Liebana J, Castillo A (2001) In vitro antibacterial activity of glass-ionomer cements. Microbios 104:141–148
- Klasen HJ (2000) A historical review of the use of silver in the treatment of burns. II. Renewed interest for silver. Burns 26:131–138. doi:10.1016/S0305-4179(99)00116-3
- Klaus T, Joerger R, Olsson E, Granqvist C-G (1999) Silver-based crystalline nanoparticles, microbially fabricated. Proc Natl Acad Sci USA 96:13611–13614. doi:10.1073/pnas.96.24.13611
- Lee DG, Kim HK, Kim SA, Park Y, Park S-C, Jang S-H et al (2003) Fungicidal effect of indolicidin and its interaction with phospholipids membranes. Biochem Biophys Res Commun 305:305–310. doi:10.1016/S0006-291X(03)00755-1
- Liao RS, Rennie RP, Talbot JA (1999) Assessment of the effect of amphotericin B on the vitality of *Candida albicans*. Antimicrob Agents Chemother 43:1034–1041
- Mares D, Romagnoli C, Sacchetti G, Vicentini CB, Bruni A (1998) Morphological study of *Trichophyton rubrum*: Ultrastructural findings after treatment with 4-amino-3-methyl-1-phenylpyrazolo-(3, 4-c) isothiazole. Med Mycol 36:379–385. doi:10.1080/02681219880000601

- Melaiye A, Sun Z, Hindi K, Milsted A, Ely D, Reneker DH et al (2005) Silver(I)-imidazole cyclophane gem-diol complexes encapsulated by electrospun terephthalic nanofibers: formation of nanosilver particles and antimicrobial activity. *J Am Chem Soc* 127:2285–2291. doi:[10.1021/ja040226s](https://doi.org/10.1021/ja040226s)
- Merisko-Liversidge E, Liversidge GG, Cooper ER (2003) Nanosizing: a formulation approach for poorly-water-soluble compounds. *Eur J Pharm Sci* 18:113–120. doi:[10.1016/S0928-0987\(02\)00251-8](https://doi.org/10.1016/S0928-0987(02)00251-8)
- Osumi M (1998) The ultrastructure of yeast: cell wall structure and formation. *Micron* 29:207–233. doi:[10.1016/S0968-4328\(97\)00072-3](https://doi.org/10.1016/S0968-4328(97)00072-3)
- Park Y, Lee DG, Jang S-H, Woo E-R, Jeong HG, Choi C-H et al (2003) A Leu-Lys-rich antimicrobial peptide: activity and mechanism. *Biochim Biophys Acta* 1645:172–182
- Silver S (2003) Bacterial silver resistance: molecular biology and uses and misuses of silver compounds. *FEMS Microbiol Rev* 27:341–353. doi:[10.1016/S0168-6445\(03\)00047-0](https://doi.org/10.1016/S0168-6445(03)00047-0)
- Sondi I, Salopek-Sondi B (2004) Silver nanoparticles as antimicrobial agent: a case study on *E. coli* as a model for Gram-negative bacteria. *J Colloid Interface Sci* 275:177–182. doi:[10.1016/j.jcis.2004.02.012](https://doi.org/10.1016/j.jcis.2004.02.012)
- Sondi I, Siiman O, Matijević E (2000) Preparation of amino-dextran-CdS nanoparticle complexes and biologically active antibody-aminodextran-CdS nanoparticle conjugates. *Langmuir* 16:3107–3118. doi:[10.1021/la991109r](https://doi.org/10.1021/la991109r)
- Sung WS, Lee I-S, Lee DG (2007) Damage to the cytoplasmic membrane and cell death caused by lycopene in *Candida albicans*. *J Microbiol Biotechnol* 17:1797–1804
- Tas J, Westerneng G (1981) Fundamental aspects of the interaction of propidium diiodide with nuclei acids studied in a model system of polyacrylamide films. *J Histochem Cytochem* 29:929–936
- Zhao GJ, Stevens SE (1998) Multiple parameters for the comprehensive evaluation of the susceptibility of *Escherichia coli* to the silver ion. *Biomaterials* 11:27–32. doi:[10.1023/A:1009253223055](https://doi.org/10.1023/A:1009253223055)